

Development, Manufacturing, and Testing of the Ariel's Structural Model Prototype Flexure Hinges



Fabio D'Anca^a, Antonio Scippa^{b,c}, Elisa Guerriero^a, Riccardo Lilli^{b,c}, Daniele Gottini^{b,c}, Paolo Picchi^{b,f}, Andrea Tozzi^b, Andrea Bocchieri^e, Enzo Pascale^e, Paolo Chioetto^{b,d}, Paola Zuppella^{b,d}, Giampaolo Preti^f, Emanuele Pace^f, Fausto Cortecchia^g, Giuseppe Malaguti^g, Emiliano Diolaiti^g, Alfonso Collura^a, Giuseppina Micela^a, Maurizio Filizzolo^h, Stefania Barbuiⁱ, Dervis Vernani^j, Marco Terraneo^j, Daniele Brienza^k, Raffaele Piazzolla^k, Mario Salatti^k, Elisabetta Tommasi^k, Andrew Caldwell^l, Paul Eccleston^l, Giovanna Tinetti^m

^aINAF-Osservatorio Astronomico di Palermo, Piazza del Parlamento 1, 90134 Palermo, Italy; ^bINAF-Osservatorio Astrofisico di Arcetri, Largo E. Fermi 5, 50125 Firenze, Italy; ^cDipartimento di Ingegneria Industriale, Università degli Studi di Firenze, Via Santa Marta, 3, 50139 Firenze, Ital; ^dCNR-Istituto di Fotonica e Nanotecnologie di Padova, Via Trasea 7, 35131 Padova, Italy; ^eDipartimento di Fisica, La Sapienza Università di Roma, Piazzale Aldo Moro 2, 00185 Roma, Italy; ^fDipartimento di Fisica ed Astronomia-Università degli Studi di Firenze, Largo E. Fermi 2, 50125 Firenze, Italy; ^gINAF-Osservatorio di Astrofisica e Scienza dello spazio di Bologna, Via Piero Gobetti 93/3, 40129 Bologna, Italy; ^hZericad di Filizzolo Maurizio, Via Alessio Narbone 66, 90138 Palermo, Italy; ⁱLaboratorio BS S.r.l., Loc. Salet, 1, 33029 Raveo UD, Italy; ^jMedia Lario S.r.l., Via al Pascolo, 10, 23842 Bosisio Parini LC, Italy; ^kASI, Agenzia Spaziale Italiana, Via del Politecnico snc, Roma, Italy; ^lRAL Space, STFC Rutherford Appleton Laboratory, Didcot, Oxon, OX11 0QX, UK; ^mDepartment of Physics and Astronomy, University College London, Gower Street, London WC1E 6BT, UK



INTRODUCTION

Ariel, the fourth medium-sized mission of ESA's "Cosmic Vision" program, was officially adopted in 2020 to comprehensively survey the atmospheres of a large sample of known exoplanets[1,2]. This mission places significant importance on critical components such as the primary mirror (M1) and its associated Flexure Hinges (FHs). FHs are not just passive mechanical-structural devices but the lifeline of the primary mirror, designed to isolate it from the mechanical and thermal effects of the Ariel Telescope's Optical Bench (TOB), thereby safeguarding its optical quality. Mechanical effects include gravity, inertial, vibratory loadings, and potential stresses resulting from integrating the primary mirror to maintain proper alignment and ensure optimal optical performance during assembly on the satellite. In this study, we underscore the pivotal role of these flexure hinges in connecting M1 to the TOB, detailing the challenges in designing and fabricating this complex structural frame and highlighting the importance of maintaining the alignment of optomechanical elements under various loads.

An essential function of FHs is to mitigate distortion effects due to shrinkage at cryogenic temperatures of 50 K. For this reason, the flexible hinges are made of the same aluminium alloy as M1 and the TOB and have undergone the same cryogenic treatments. Fig.1 shows an exploded view with all the components and how the FHs are positioned on M1.

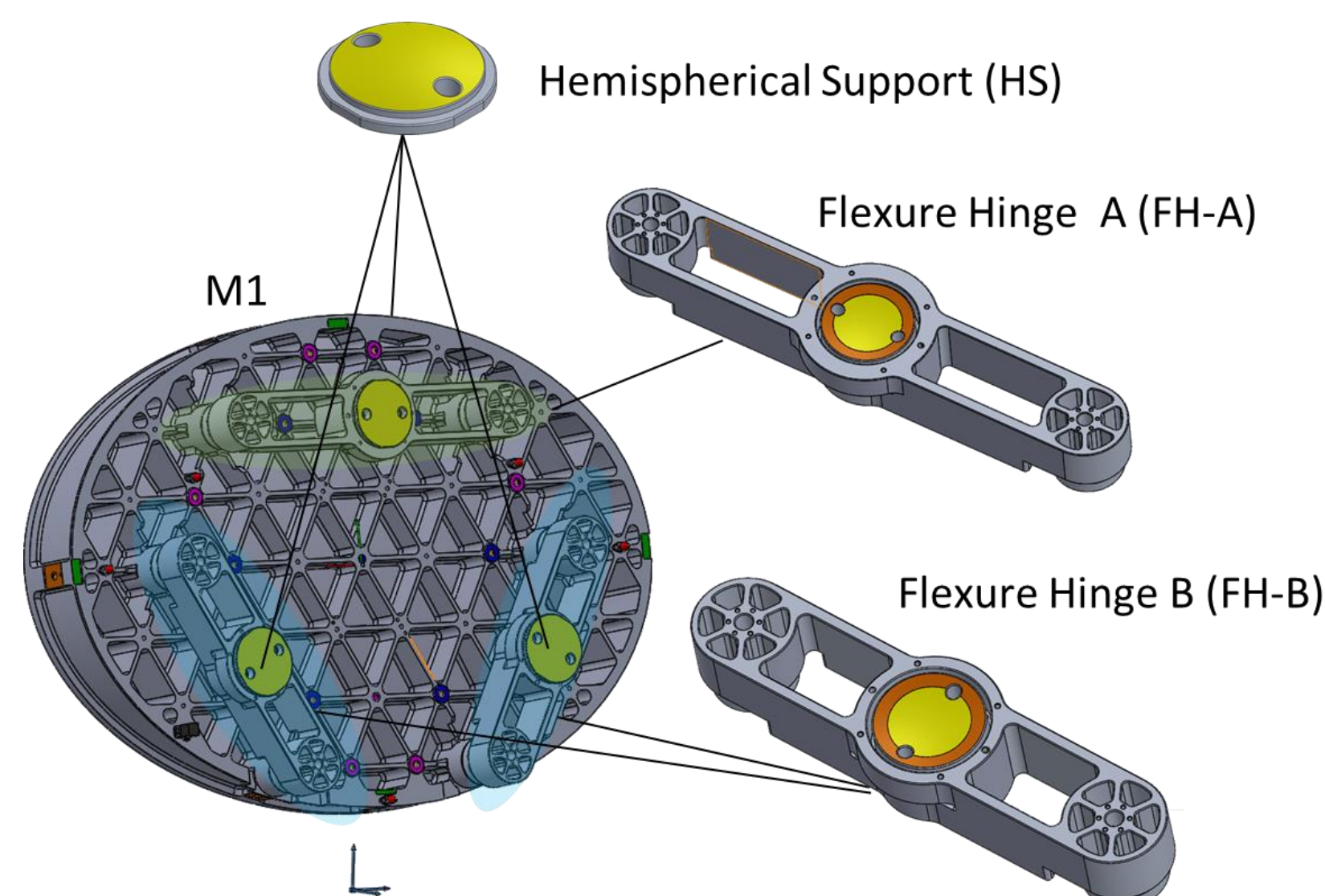


Fig.1 - Explode view of M1 and Flexure Hinges.

Three FHs of two types support the M1 mirror on its back (see Fig.2). They are mounted to form a triangular configuration with the centre of the mirror's centre of mass.

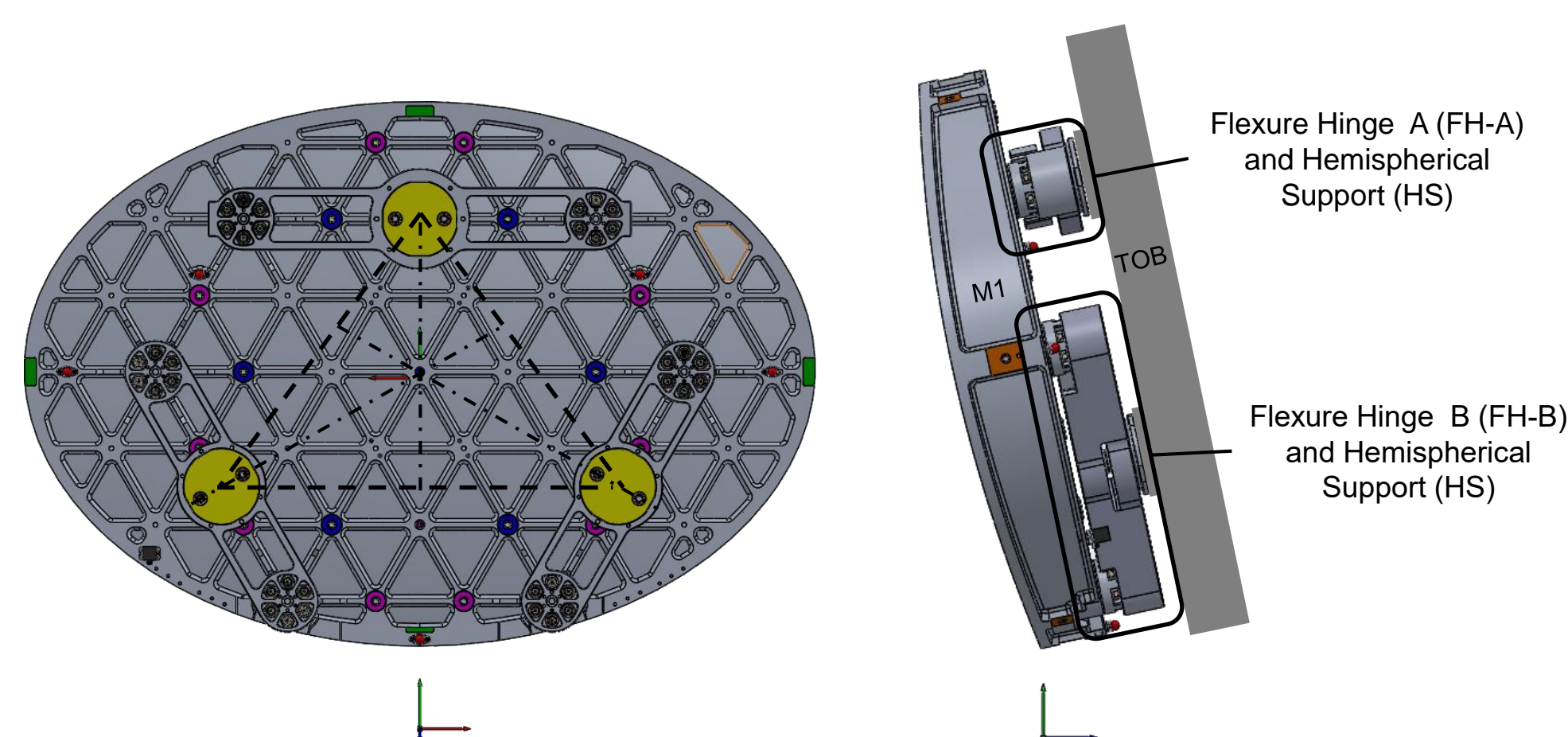


Fig.2 - Assembly schema of FHs on M1 and TOB.

To minimize distortion of M1 due to mounting the flexible hinges on M1, the manufacturing tolerances of the interface planes of both components were set at 2 µm flatness.

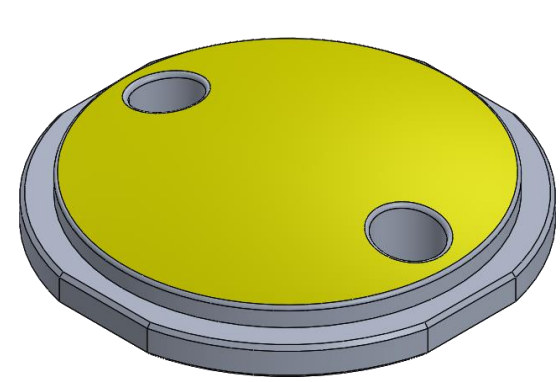


Fig.3 - Hemispherical Support (HS) with a sphere R 195 mm.

The mechanical coupling between the HS (see Fig.3) and the FH is achieved through the interaction of a sphere and a conical-spherical housing surface generated on the FH. When coupled with the sphere of the HS during the assembly phase, this conical-spherical surface ensures optimal sliding of the two parts. When the two surfaces are subjected to the load of the tightening screws, the minimal clearance obtained through tolerances should enable the best possible thermal contact.

MANUFACTURING

The manufacture of the FHs involved high-precision machining techniques, from milling to Electrical Discharge Machining (EDM) and Single-Point Diamond Turning (SPDT). Milling was performed with a three-axis machine with mechanical masking and precision-calibrated shims to avoid plastic deformation during flexure machining. The complexity of the flexure hinges stems from the need to provide multiple degrees of freedom during installation to compensate for manufacturing errors and the different spring parts capable of mitigating stresses due to the vibration load levels. The more flexible parts of FHs (flexors) are also needed to reduce stresses at the interface with M1 and TOB due to the action of gravity and thermomechanical stresses caused by temperature gradients during the cooling phase[3]. In particular, the flexural hinge stiffnesses of the parts are: K_1 , cylindrical under HS, functions as an elastic spherical hinge to help compensate for any jamming due to cone-sphere contact during assembly (Fig.4). At the same time, K_2 allows the central body to translate, compensating for differential contractions between TOB and M1[4].

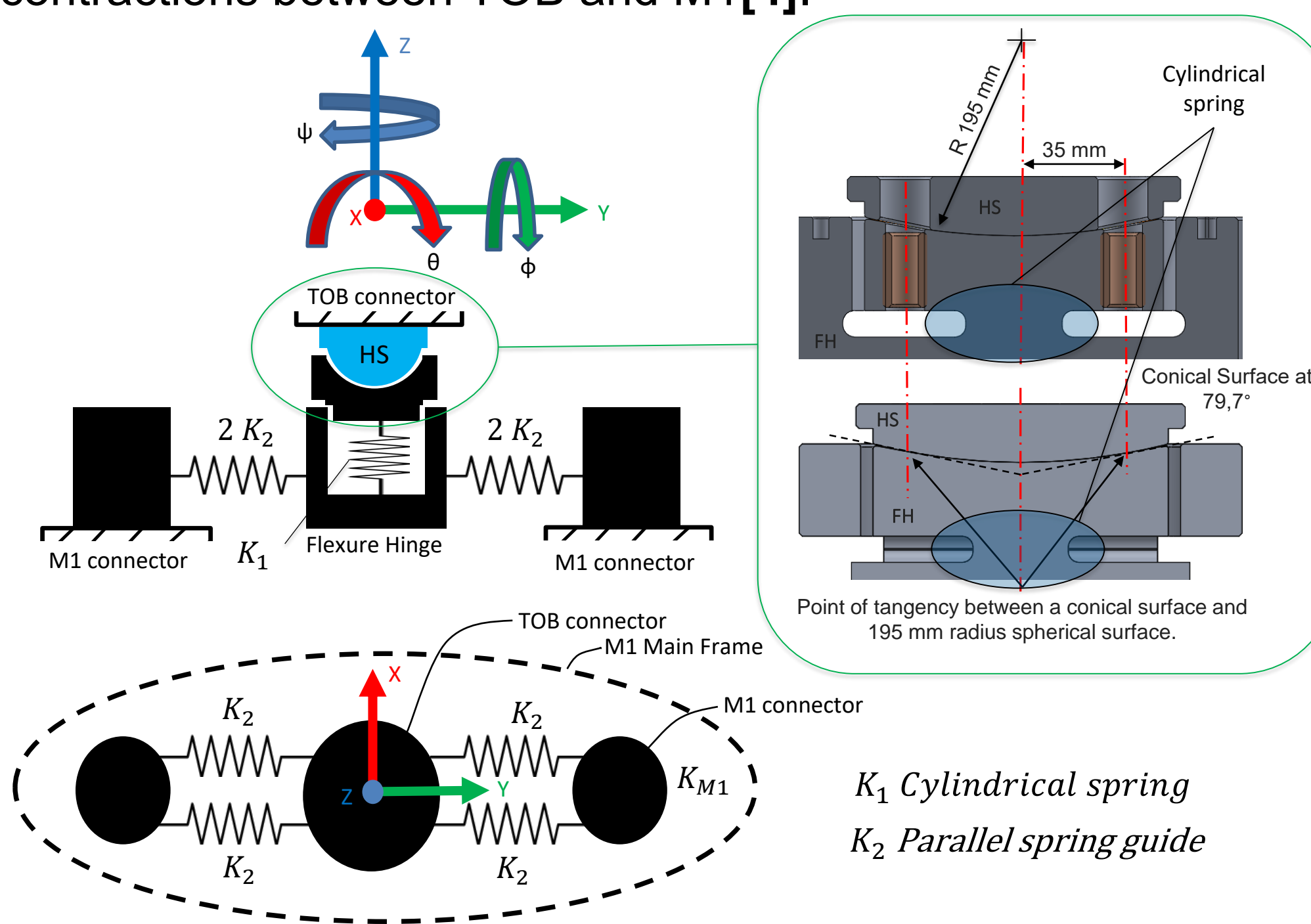


Fig.4 - general Flexure Hinges schema and coupling between FH and HS component.

Modal Analysis

The finite element analysis (FEA) allowed the determination of the resonance frequencies and the natural shape assumed by the FH-A prototype. The first mode is lateral bending on the Z-axis and translation on the X-axis. With a higher frequency, the second mode is a rotation around the X-axis and translation in the Z-axis. The third mode is a rotation around the Y-axis. These first three resonance modes, illustrated in Fig.5, originate from the three natural frequencies of the parallel spring guides. The modes generated by the central cylindrical spring appear above 1000 Hz, demonstrating high bending and torsional stiffness.

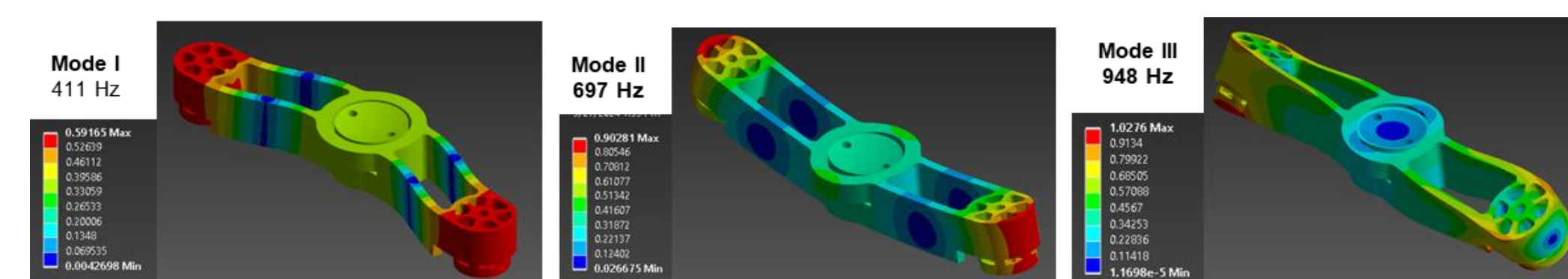


Fig.5 - Modal analysis of FH-A prototype.

Milling machines process
Milling was performed with a three-axis machine, using jigs and shims to avoid plastic deformation during flexure machining.

Fig.6 - General phase of milling.

Plunge Electrical Discharge Machining (EDM) process
Start at the end of the milling phase with 0.6 mm extra material for rough machining at 15 A. Continue with 0.4 mm extra material for semi-finishing at 9 A, then proceed with 0.2 mm extra material for finishing at 4 A. Finally, use 0.05 mm extra material for high finishing at 1.5 A

Fig.7 - Phase of EDM of the cylindrical flexor.

Single-Point Diamond Turning (SPDT) process
SPDT was used to obtain the co-coplanarity 2 µm surfaces of the two interface pads with M1. The cone-sphere surface was also made by SPDT. The surface roughness of all machined surfaces must be below 0.2 µm, and the form tolerance is ±4 µm.

Fig.8 - Phase of SPDT a) is the interface between the FH and the Lathe spindle b) the FH-A mounted on the Lathe c) is the interface between HS and the Lathe spindle d) the HS mounted on the Lathe.

RESULTS

MANUFACTURING QUALITY

The development of an FH prototype was aimed at verifying the feasibility in terms of machining and compliance with the project's stringent dimensional and shape tolerances. Additionally, the construction of the Flexure Hinge type A (FH-A) prototype allowed for verification of its actual functionality once mounted on the M1 Structural Model (SM) mirror, a mirror used for structural tests but with optical properties.

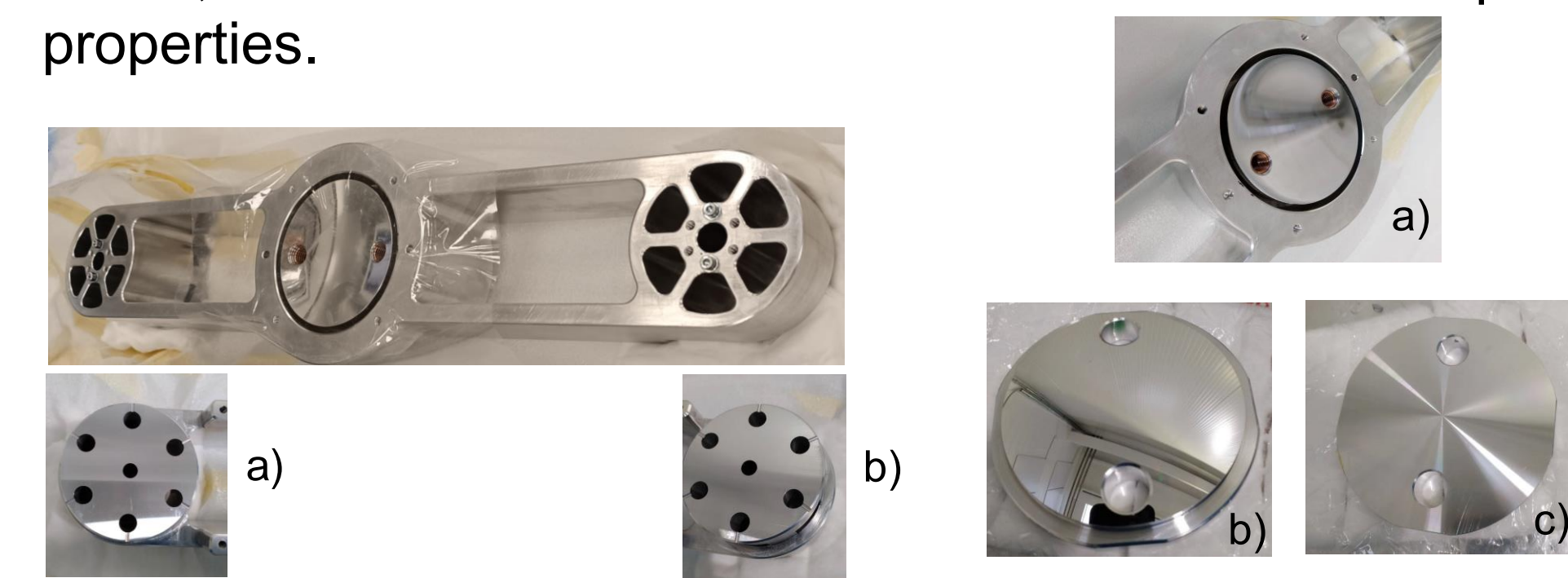


Fig.9 - Mock-up of Flexure Hinges (FH) A: Images a) and b) show the surface quality achieved on the pads.

The SPDT machining process of the two pads of the FH (see Fig.9) has allowed achieving a flatness of less than 2 µm, while maintaining the design specifications.

Fig.10 - Mock-up of hemispherical support (HS): Image a) shows the quality of the spherical-conical surface of the HS housing made on the FH, b) shows the quality of the spherical surface of the HS, and c) shows the quality of the flat surface of the HS.

The tight tolerance of ±5 µm on the fitting dimensions between the FH housing and the HS (see Fig.10) has been respected.

TEST

The performance of the M1 SM mirror was evaluated by installing a prototype of the FH-A and measuring the Surface Form Error (SFE) before and after assembly.

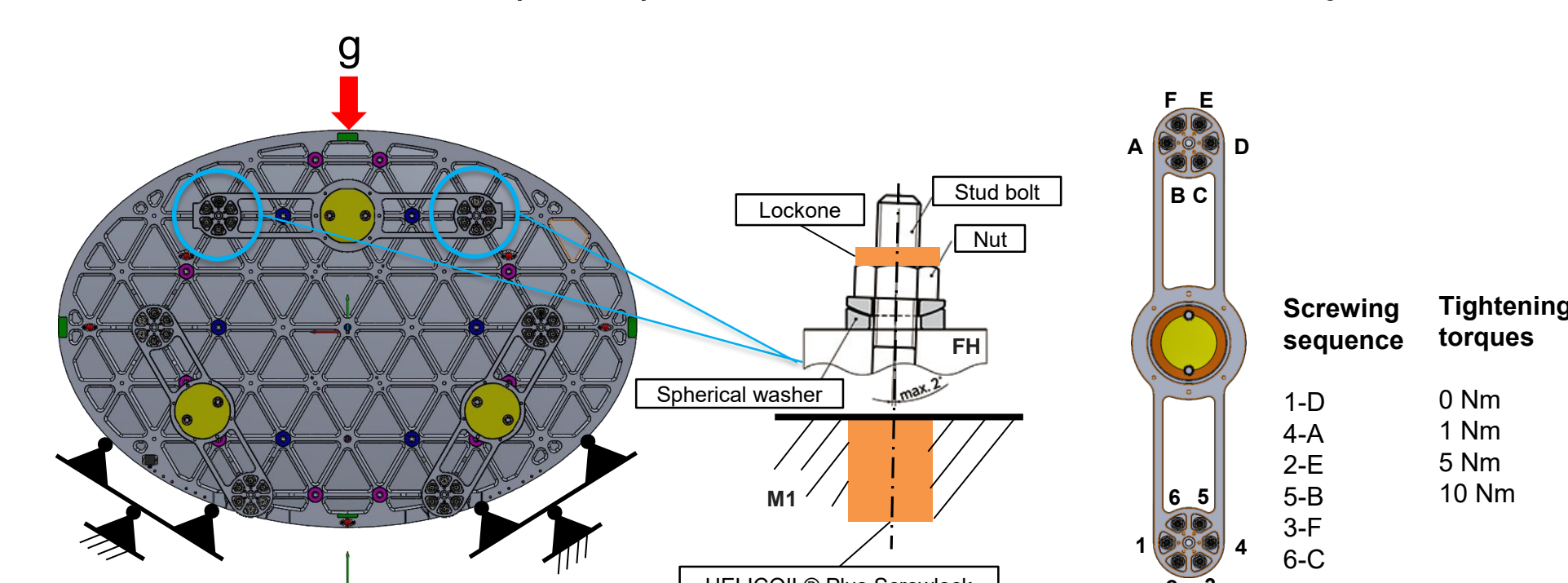


Fig.11 - M1 SM (1 m class) undergoing testing with only the FH-A mounted.

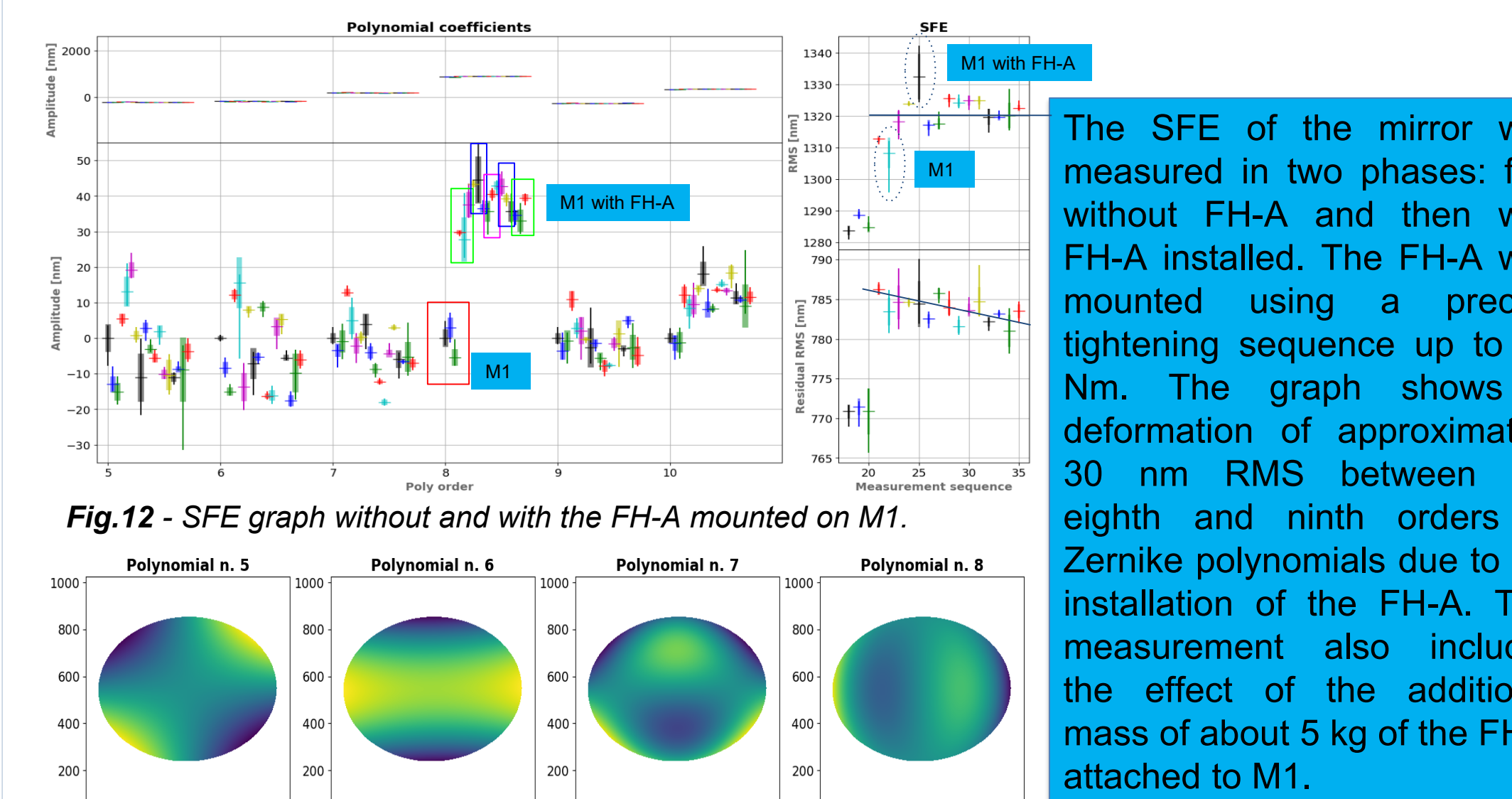


Fig.12 - SFE graph without and with the FH-A mounted on M1.

Fig.13 - SFE maps aberrations of the M1 mirror starting from the Zernike polynomial from 5 to 8 with FH-A mounted.

The SFE of the mirror was measured in two phases: first without FH-A and then with FH-A installed. The FH-A was mounted using a precise tightening sequence up to 10 Nm. The graph shows a deformation of approximately 30 nm RMS between the eighth and ninth orders of Zernike polynomials due to the installation of the FH-A. This measurement also includes the effect of the additional mass of about 5 kg of the FH-A attached to M1.

ACKNOWLEDGEMENTS

The activities described in this paper are being developed under the Implementation Agreement n. 2021-5-HH.2-2024 "Italian Participation to Ariel mission phase B2/C" between the Italian Space Agency (ASI) and the National Institute for Astrophysics (INAF) and under ASI contracts n. 2021-21-I.0 "ARIEL TA Phase B Industrial Activities" and n. 2023-42-I.0 "ARIEL TA Phase C/D1 Industrial Activities".

REFERENCES

- Turon, C., "Esa space science programme, cosmic vision 2015-2025, for astrophysics," Proceedings of The International Astronomical Union 2 (08 2007).
- Tinetti, G., Drossart, P., Eccleston, P., Hartogh, P., Heske, A., Leconte, J., Micela, G., Ollivier, M., Pilbratt, G., Turrini, D., Vandenbussche, B., Wolkenberg, P., Pascale, E., Beaulieu, J.-P., G'udel, M., Rataj, M., Ray, T., Ribas, I., and Zapatero-Osorio, M., "The science of Ariel (atmospheric remote-sensing infrared exoplanet large-survey)," 99041X (07 2016).
- ARIEL ASSESSMENT STUDY REPORT "YELLOW BOOK", Publication date: 01 March 2017, Page: 1-110, Year: 2017, Reference: ESA/SCI(2017)2.
- Daniel Vukobratovich, Ralph M. Richard, "Flexure mounts for high -resolution optical elements" SPIE Vol. 959 Optomechanical and Electro-Optical Design of Industrial Systems (1988).